Remote sensing space weather events: Antarctic-Arctic Radiation-belt (Dynamic) Deposition-VLF Atmospheric Research Konsortium network

Mark A. Clilverd,[1] Craig J. Rodger,[2] Neil R. Thomson,[2] James B. Brundell,[3] Thomas Ulich,[4] János Lichtenberger,[5] Neil Cobbett,[1] Andrew B. Collier,[6,7] Frederick W. Menk,[8] Annika Seppälä,[1,9] Pekka T. Verronen,[9] and Esa Turunen[4]

Received 9 May 2008; revised 7 November 2008; accepted 15 December 2008; published 2 April 2009.

[1] The Antarctic-Arctic Radiation-belt (Dynamic) Deposition-VLF Atmospheric Research Konsortium (AARDDVARK) provides a network of continuous long-range observations of the lower ionosphere in the polar regions. Our ultimate aim is to develop the network of sensors to detect changes in ionization levels from ~30–90 km altitude, globally, continuously, and with high time resolution, with the goal of increasing the understanding of energy coupling between the Earth's atmosphere, the Sun, and space. This science area impacts our knowledge of space weather processes, global atmospheric change, communications, and navigation. The joint New Zealand-United Kingdom AARDDVARK is a new extension of a well-established experimental technique, allowing long-range probing of ionization changes at comparatively low altitudes. Most other instruments which can probe the same altitudes are limited to essentially overhead measurements. At this stage AARDDVARK is essentially unique, as similar systems are only deployed at a regional level. The AARDDVARK network has contributed to the scientific understanding of a growing list of space weather science topics including solar proton events, the descent of NO_x into the middle atmosphere, substorms, precipitation of energetic electrons by plasmaspheric hiss and electromagnetic ion cyclotron waves, the impact of coronal mass ejections upon the radiation belts, and relativistic electron microbursts. Future additions to the receiver network will increase the science potential and provide global coverage of space weather event signatures.

Citation: Clilverd, M. A., et al. (2009), Remote sensing space weather events: Antarctic-Arctic Radiation-belt (Dynamic) Deposition-VLF Atmospheric Research Konsortium network, *Space Weather*, *7*, S04001, doi:10.1029/2008SW000412.

1. Introduction

[2] The Antarctic-Arctic Radiation-belt (Dynamic) Deposition-VLF Atmospheric Research Konsortium (AARDDVARK) is a global network of radio receivers designed to make continuous long-range observations of the lower ionosphere at mid to high-latitude regions. The network of cheap, easy to install, easy to maintain sensors use preexisting man-made very low frequency radio waves (VLF) to detect changes in ionization levels from ~30–90 km altitude, continuously, and with high time resolution. The network's goal is to increase the understanding of energy coupling between the Earth's atmosphere, the Sun, and space. The part of the electromagnetic spectrum described as VLF generally spans 3–30 kHz. Most ground-based observations in the VLF band are dominated by the strong impulsive signals radiated by lightning discharges. These produce significant electromagnetic power from a few hertz to several hundred megahertz [*Magono*, 1980], with the bulk of the energy radiated in the VLF frequency band. At VLF such pulses are termed "atmospherics," or simply "sferics." In addition to sferics, at frequencies >10 kHz man-made transmissions from communication and navigation transmitters can be observed in almost every part of the world.

[1]Physical Sciences Division, British Antarctic Survey, Cambridge, UK.
[2]Department of Physics, University of Otago, Dunedin, New Zealand.
[3]UltraMSK.com, Dunedin, New Zealand.
[4]Sodankylä Geophysical Observatory, University of Oulu, Sodankylä, Finland.
[5]Space Research Group, Eötvös University, Budapest, Hungary.
[6]Hermanus Magnetic Obsevatory, Hermanus, South Africa.
[7]School of Physics, University of KwaZulu Natal, Durban, South Africa.
[8]School of Mathematical and Physical Sciences and Cooperative Research Centre for Satellite Systems, University of Newcastle, Callaghan, New South Wales, Australia.
[9]Earth Observation, Finnish Meteorological Institute, Helsinki, Finland.

[3] Most of the energy radiated by man-made VLF transmitters is trapped between the conducting ground (land, sea, or ice) and the lower part of the ionosphere, forming the Earth-ionosphere waveguide. Such radiation is said to be propagating ''subionospherically,'' i.e., beneath the ionosphere. At wavelengths of about 15 km ($\sim$20 kHz) all the antennas are electrically short and therefore have low-radiation efficiency. However, operationally this is compensated for by having very high input powers, making these transmitters expensive to run. As a result the creation and operation of man-made VLF transmitters is generally due to military requirements. Nevertheless, the scientific use of the transmissions from these stations has a long and successful history. Following the invention of radio wave transmission and reception [*Popov*, 1896] Heaviside and Kennelly [*Kennelly*, 1902] postulated the existence of what we now know as the ionosphere in order to explain the observed reflection of radio waves. Using a technique developed by *Hollingworth* [1926] of making VLF recordings as a function of range, VLF transmitter signals were shown to exhibit an interference pattern, which could be compared with theoretical estimates [*Weeks*, 1950]. In the subionospheric waveguide the upper and lower boundaries strongly affect the propagation conditions for the VLF waves. As the conducting ground (land, sea, or ice) is essentially unchanging with time it is the upper boundary that drives most of the temporal variability in the amplitude and phase of man-made transmitters observed from a distant location. The upper boundary of the waveguide is the ionized D region at $\sim$70–85 km, and shows variations caused by local changes in ionization rates at altitudes below the D region caused by space weather events. During undisturbed conditions the amplitude and phase of fixed frequency VLF transmissions varies in a consistent way and thus space weather events can be detected as deviations from the ''quiet day curve.'' For a much more comprehensive review of this topic we refer the reader to the discussion by *Barr et al.* [2000] which highlights the development of VLF radio wave propagation measurements particularly over the last 50 years.

[4] In order to interpret any observed fluctuations in a received VLF signal it is necessary to reproduce the characteristics of the deviations using mathematical descriptions of VLF wave propagation [e.g., *Sommerfeld*, 1909; *Budden*, 1955; *Wait*, 1963], and thus determine the ionization changes that have occurred around the upper waveguide boundary. This was the challenge during the early days of the subject. Some 50 years ago the early work of *Piggott et al.* [1965] and *Pitteway* [1965] focused on observations from single frequency radio links between Rugby and Cambridge, UK, for example, those observations made by *Bracewell et al.* [1951] and *Straker* [1955]. One successful approach of the time was to determine the D region electron concentration altitude profile using a systematic application of trial and error in order to reproduce the observations [e.g., *Hollingworth*, 1926; *Deeks* 1966a, 1966b]. This approach worked best with observations at many frequencies and transmitters sites, and many receiving sites in order to determine the spatial structure, and electron concentration altitude profile of the ionization enhancement region. Essentially this approach is still used today, where ionization effects on VLF wave propagation can be modeled using powerful programs such as the Long Wave Propagation Code (LWPC) [*Ferguson and Snyder*, 1990]. LWPC models VLF signal propagation from any point on Earth to any other point. Given electron density profile parameters for the upper boundary conditions, LWPC calculates the expected amplitude and phase of the VLF signal at the reception point. The code models the variation of geophysical parameters along the path as a series of horizontally homogeneous segments. To do this, the program determines the ground conductivity, dielectric constant, orientation of the geomagnetic field with respect to the path and the solar zenith angle, at small fixed distance intervals along the path. Given electron density profile parameters for the upper boundary conditions for each section along the path, LWPC calculates the expected amplitude and phase of the VLF signal at the reception point. Thus it can be used to investigate the modification of the ionosphere during precipitation events driven by space weather, characterizing the electron density profile produced by the precipitating particles. A limitation of this technique is in the inability to determine if all, or if only part of, a transmitter-receiver path is affected by the precipitating particles. This can be overcome by using multiple, crossing paths, and data from other instruments (such as riometers) or satellite observations.

[5] Although much work has previously been done in this area of science, and many observations of space weather effects have been interpreted using data collected over many years, we now have the advantage of direct satellite observations of the conditions occurring in the radiation belts, magnetosphere, and even close to the Sun, in addition to powerful VLF modeling capabilities. Thus we are able to use in situ, single-point satellite measurements of space weather events to contextualize the AARDDVARK network observations. Hence we can broaden the satellite contribution and provide key parameters missing from the ''satellite picture,'' i.e., duration of an event, occurrence frequency, spatial structure, energy spectra, energy flux, depending on which is most difficult to measure from space and which may be determined through trial and error analysis of AARDDVARK data.

[6] Because of the frequencies at which man-made naval transmitters broadcast, allied to their high radiated power (typically ranging from 50 kW to 1 MW), and their nearly continuous operation, they are extremely well suited to long-range remote sensing of the lower ionosphere, probably the least studied region of the Earth's atmosphere. These altitudes ($\sim$50–90 km) are too high for balloons and too low for most satellites, making in situ measurements extremely rare. Rocket lofted experiments

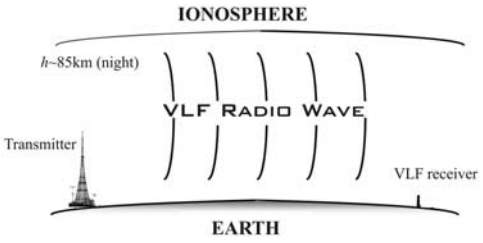

Figure 1. Schematic of subionospheric VLF propagation. The vast majority of the energy in VLF transmissions propagate in the waveguide formed by the Earth and the lower edge of the ionosphere (for nighttime ~85 km).

have taken place in the D region, but can only provide limited coverage because of their very nature. Radio soundings made at frequencies >1 MHz (e.g., ionosondes), while successful for observing the upper ionosphere, generally fail in the D region. The low electron number densities at D region altitudes produce weak reflections, and hence measurement difficulties, particularly at night.

[7] Observations of the amplitude and/or phase of VLF transmissions have provided information on the variation of the D region, both spatially and temporally. A schematic of subionospheric propagation is shown in Figure 1. The nature of the received radio waves is largely determined by propagation between the Earth-ionosphere boundaries [e.g., *Cummer*, 2000]. Very long-range remote sensing is possible; these signals can be received thousands of kilometers from the source as shown in the results published by *Round et al.* [1925], *Bichel et al.* [1957], *Crombie* [1964], and many others (we direct the reader to the excellent summary by *Watt* [1967, chapter 3]). In contrast, incoherent scatter radar techniques can make measurements in the D region and above [e.g., *Turunen et al.*, 1996], but are limited to essentially overhead measurements. By using multiple VLF communication transmitters some understanding has been gained of both the daytime lower ionosphere [*McRae and Thomson*, 2000], and the nighttime lower ionosphere [*Thomson et al.*, 2007], particularly in terms of how to model it accurately through programs such as LWPC. Because of the complex nature of the nighttime lower ionosphere, or during disturbed conditions, a much larger number of transmitter–receiver paths are required. The most efficient and cost effective method is to use existing transmitters and deploy a large array of receivers [e.g., *Bainbridge and Inan*, 2003]. We expand upon this approach to a wider range of science questions using the Antarctic Arctic Radiation-belt (Dynamic) Deposition VLF Reasearch Konsortia network which, operating in the polar regions, is providing promising results on a number of active space weather science topics such as: Solar Proton Events, Relativistic Electron Precipitation, Descent of NO_x from Thermospheric Altitudes, and Solar Flares. We introduce each one of these science areas in turn below, before describing the AARDDVARK network in detail, and the recent contributions which have flowed from its observations. AARDDVARK data variations can be produced by multiple space weather drivers. However, with the context provided by other ground-based and satellite data sets, as well as signatures in the AARDDVARK observations themselves, we can determine the dominant space weather driver, and hence focus on the physics of the particular situation. This is described below.

1.1. Solar Proton Events

[8] Processes on the Sun can accelerate protons to relativistic energies, producing Solar Proton Events (SPE), also known as Solar Energetic Particle (SEP) events. Arguments continue as to whether the acceleration is driven by the X-ray flare release process or in solar wind shock fronts during coronal mass ejections [*Krucker and Lin*, 2000; *Cane et al.*, 2003]. The high-energy component of this proton population is at relativistic levels such that they can reach the Earth within minutes of solar X-rays produced during any solar flares which may be associated with the acceleration. Satellite data show that the protons involved have an energy range spanning 1 to 500 MeV, occur relatively infrequently, and show high variability in their intensity and duration [*Shea and Smart*, 1990]. For large events the duration is typically several days, with risetimes of ~1 h, and a slow decay to normal flux values thereafter [*Reeves et al.*, 1992]. SPE particles cannot access the entire global atmosphere as they are partially guided by the geomagnetic field, such that their primary impact is upon the polar atmosphere. The SPE effect on VLF propagation in the polar regions is large and often observed as a massive attenuation of the wave amplitudes lasting several days. The events can be recognized in part because of their close time correlation with satellite proton flux data (i.e., GOES spacecraft), and in part because of a very smooth lower ionosphere boundary reducing short timescale variability in the AARDDVARK amplitude and phase data. SPEs can cause significant changes in the chemical balance of the atmosphere and work is currently underway to quantify these effects, as described below.

1.2. Relativistic Electron Precipitation

[9] At geostationary orbits geomagnetic storms have been found to cause significant variations in trapped radiation belt relativistic electron fluxes, through a complex interplay between competing acceleration and loss mechanisms. *Reeves* [1998] found that geomagnetic storms produce all possible responses in the outer belt flux levels, i.e., flux increases (53%), flux decreases (19%), and no change (28%). Understanding the loss of relativistic electrons is a key part to understanding the dynamics of the energetic radiation belts. Flux decrease events usually begin in the premidnight sector (1500–2400 MLT), and typically show decreases in >2 MeV electron flux within a few hours of onset, followed by an extended period of low flux suggesting permanent electron loss. A significant loss

mechanism that removes trapped relativistic electrons from the radiation belts is Relativistic Electron Precipitation (REP) into the atmosphere. REP has been observed to take several forms, one of which is relativistic microbursts which are bursty, short-duration (<1 s) precipitation events containing electrons of energy >1 MeV [*Imhof et al.*, 1989; *Blake et al.*, 1996], as well as another form which is prolonged precipitation lasting minutes to hours [*Millan et al.*, 2002]. The relative significances of the loss mechanisms are currently being investigated. The REP effect on VLF propagation in the polar regions is highly variable, being either increases or decreases in amplitude or phase or both, and therefore difficult to determine if it is REP that is occurring from the data alone. However, these events can be recognized in part because of their close time correlation with elevated geomagnetic activity indices, where often they occur with sudden onset signatures, and in part when there is a lack of coincident SPE effects in the AARDDVARK data.

1.3. Descent of NO_x From Thermospheric Altitudes

[10] Winter time polar odd Nitrogen, NO_X (NO + NO_2), is produced at high altitudes in the thermosphere and the mesosphere. During periods of efficient vertical transport inside the polar vortex the NO_X can descend to the stratosphere [*Solomon et al.*, 1982a; *Siskind*, 2000]. In the upper mesosphere the NO_X is mainly in the form of NO; as the NO_X descends it is converted to NO_2 [*Solomon et al.*, 1982a]. NO_X plays a key role in the Ozone balance of the middle atmosphere because it destroys odd oxygen (O + O_3) through catalytic reactions [e.g., *Brasseur and Solomon*, 2005, pp. 291–299]. Hard energetic particle precipitation (EPP) into the mesosphere (that including a significant population of >100 keV electrons and >1 MeV protons), and softer EPP into the thermosphere (<100 keV electrons), generate in situ enhancements in odd nitrogen. The mesospheric source is dominated by strong impulsive ionization episodes such as solar proton events [*Verronen et al.*, 2005], while the thermospheric source is more continuous, being dominated by auroral ionization [*Siskind*, 2000]. Chemical changes driven by the ionization of the neutral atmosphere influence the ozone profile both in the mesosphere and the stratosphere and therefore stratospheric temperatures and dynamics. Thus the observation of significant levels of NOx in the polar atmosphere is a topic of significant debate in terms of atmospheric forcing.

[11] Subionospheric VLF radio wave propagation is sensitive to ionization located below about 90 km, including that produced by the ionization of descending NO_X by Lyman-α [*Solomon et al.*, 1982b]. From the changes in ionospheric propagation conditions during the winter period elements of the AARDDVARK network can be used to determine the levels of mesospheric NO_X either through in situ production or descent from the thermosphere. The effect of NO_X ionization enhancements on VLF propagation in the polar regions is variable depending on the specific propagation path being studied. On many paths the influence of changing NO_X is small and virtually undetectable. However, on a few paths there are subtle multiday changes in the quiet day curve that coincide with changes in chemical composition measurements made by satellites such as ENVISAT and SABRE. In addition, the NO_X descent effect lasts for $\sim$10 days, and hence is easily differentiated from other much more short-lived drivers (e.g., particle precipitation). The combination of satellite and AARDDVARK data has improved understanding of event timing, and altitude resolution.

1.4. Solar X-Ray Flares

[12] During solar flares the X-ray flux received at the Earth increases dramatically, often within a few minutes, and then decays again in times ranging from a few tens of minutes to several hours. These X-rays have major effects in the Earth's upper atmosphere but are absorbed before they reach the ground. X-ray detectors on the GOES satellites have been recording the fluxes from solar flares since about 1976. During the very largest flares, such as the great flare of 4 November 2003, the GOES detectors saturate, resulting in considerable uncertainty as to the value of the peak X-ray flux. However, flare-induced ionospheric changes show no saturation effects thus allowing the ionosphere to be used a huge detector. Measurements of VLF phase changes monitored by elements of the AARDDVARK network have been used to extrapolate the GOES X-ray fluxes (0.1–0.8 nm) beyond saturation, e.g., to calculate the peak of the great X45 flare using daytime VLF paths across the Pacific to Dunedin, New Zealand [*Thomson et al.*, 2004]. The X-ray flare effect on VLF propagation in the polar regions can be recognized because of their close time correlation with elevated X-ray fluxes reported from satellites (e.g., GOES). The phase changes caused by the extra ionization generated by the flares are particularly well correlated with the flare flux levels, and thus phase changes are used in AARDDVARK-based studies in preference to amplitude changes.

[13] In this paper we describe the AARDDVARK network in detail, highlight the science undertaken so far, and the progress made in the areas of space weather research. We also describe the potential for integration with other experimental data sets, and the coupling to atmospheric modeling efforts.

2. Experimental Setup

[14] The AARDVARK network currently uses narrow band subionospheric VLF/LF data spanning 10–40 kHz received at ten sites: Table 1 lists the receiver site geographic coordinates, and geomagnetic *L* shell. These sites are part of the Antarctic-Arctic Radiation-belt Dynamic Deposition VLF Atmospheric Research Konsortia (see the description of the instruments, propagation paths, data policy, publications, presentations, and much more at www.physics.otago.ac.nz/space/AARDDVARK_homepage.htm). Each receiver is capable of receiving multiple narrowband transmissions

Table 1. AARDDVARK Receiver Site Locations, Geographic Coordinates, and Geomagnetic *L* Shells[a]

Site	Latitude	Longitude	*L* Shell (2008)
Northern Hemisphere			
Ny Ålesund (BAS)	78° 54′ N	11° 53′ E	∞
Churchill (BAS)	58° 45′ N	94° 54′ W	7.6
Sodankylä (SGO)	67° 22′ N	26° 23′ E	5.2
Cambridge (BAS)	52° 18′ N	00° 00′ E	2.3
Erd (Eötvös University)	48° 00′ N	19° 00′ E	1.9
Southern Hemisphere			
Casey (AAD and BAS)	66° 18′ S	110° 30′ E	∞
Scott Base (Otago and ANZ)	77° 50′ S	166° 39′ E	32
Halley (BAS)	75° 30′ S	26° 54′ W	4.5
Sanae (University of KwaZulu Natal)	72° 00′ S	01° 00′ W	4.6
Marion Is. (University of KwaZulu Natal)	46° 55′ S	37° 45′ E	2.9
Rothera (BAS)	67° 30′ S	68° 06′ W	2.8
Dunedin (Otago)	45° 47′ S	170° 28′ E	2.7

[a]BAS, British Antarctic Survey; SGO, Sodankylä Geophysical Observatory; AAD, Australian Antarctic Division; Antarctica New Zealand.

from powerful man-made communication transmitters. Table 2 lists some of the transmitters that are regularly monitored by the AARDDVARK network. The overall pattern of transmitters and receivers is shown in Figure 2. Most of our AARDDVARK sensors are deployed to monitor the Antarctic and Arctic regions, although the plot shows that many paths could be used for more equatorial studies if required. The great circle paths between the monitored VLF communications transmitters (T_x, circles) and the existing AARDDVARK receiver locations (R_x, red diamonds) are shown, indicating the atmospheric areas monitored. The AARDDVARK sensors we plan to add to the array in the near future are shown as yellow squares. The effects of changing ionization conditions in the mesosphere, often due to energetic particle precipitation, can be observed along the propagation path between a transmitter and a receiver. The effect of increased ionization on the propagating signals can be seen as either an increase or decrease in signal amplitude or phase depending on the modal mixture of each signal observed [*Barr et al.*, 2000]. In detailed modeling of any space weather effects it is important to be able to accurately reproduce any phase change as well as amplitude change observed, in order to provide a correct interpretation of the phenomenon. In this paper we preferentially show amplitude observations and modeling results, although in the appropriate papers referenced in the text we also reproduce the phase changes where possible. Amplitude variations are shown preferentially primarily because when undertaking analysis of multiday periods it is not always possible to be sure if some of the observed phase changes are due to geophysical, instrumental, or transmitter effects.

[15] The AARDDVARK network was formed in January 2005. However, some of the sensors which make up the network were individually operational well before this date, while others have come online since. The instrumentation involved is relatively cheap, simple, and easy to maintain. The majority of the receiving systems measure both the phase and amplitude of MSK modulated narrowband VLF radio signals, with the demodulation increasingly implemented in software running on standard PC hardware. Operational AARDDVARK sensors vary from location to location. The majority are currently based upon the "OmniPAL" narrowband VLF receiver [*Dowden et al.*, 1998]. Currently, AARDDVARK sensors include the following receiver types: OmniPAL (and its absolute phase upgrade "AbsPAL"), UltraMSK and VELOX AARDDVARK. The receivers are capable of recording the amplitude and phase of Minimum Shift Keying (MSK) modulated VLF radio transmissions. Each of these systems requires a front end aerial and preamplifier. The aerial is typically a vertical magnetic loop antenna, preferably two orientated orthogonally as the loops are directional. Individual transmitter signals are monitored on either loop depending on the direction of the transmitter from the receiver site. The similarities and differences of the three primary types of instrument are described briefly below.

[16] The OmniPAL narrowband VLF receiver is a software defined radio (SDR) system [*Adams and Dowden*,

Table 2. VLF Transmitter Call Signs, Frequency, Geographic Coordinates, Output Power, and Geomagnetic *L* Shells

Transmitter	Frequency (kHz)	Latitude	Longitude	Estimated Power (kW)	*L* Shell (2008)
NRK, Iceland	37.5	63° 51′ N	22° 28′ W	100	5.5
NLK, Seattle	24.8	48° 12′ N	121° 55′ W	250	2.9
NDK, North Dakota	25.2	46° 22′ N	98° 20′ W	500	3.3
NAA, Maine	24.0	44° 39′ N	67° 17′ W	1000	2.9
GQD, Anthorn	22.1	54° 53′ N	03° 17′ W	60	2.7
HWU, Rosnay	22.6	46° 43′ N	01° 15′ E	200	1.8
DHO, Ramsloh	23.4	53° 05′ N	07° 37′ E	300	2.4
ICV, Tavolara Island	20.27	40° 55′ N	09° 45′ E	50	1.5
NWC, NW Cape	19.8	21° 49′ S	114° 10′ E	1000	1.4
NTS, Woodside	18.6	38° 29′ S	146° 56′ E	25	2.4
NPM, Hawaii	21.4	21° 26′ N	158° 09′ W	500	1.2
NAU, Puerto Rico	40.75	18° 25′ N	67° 09′ W	125	–
JAP, Ebino	22.2	32° 03′ N	130° 50′ E	100	1.2

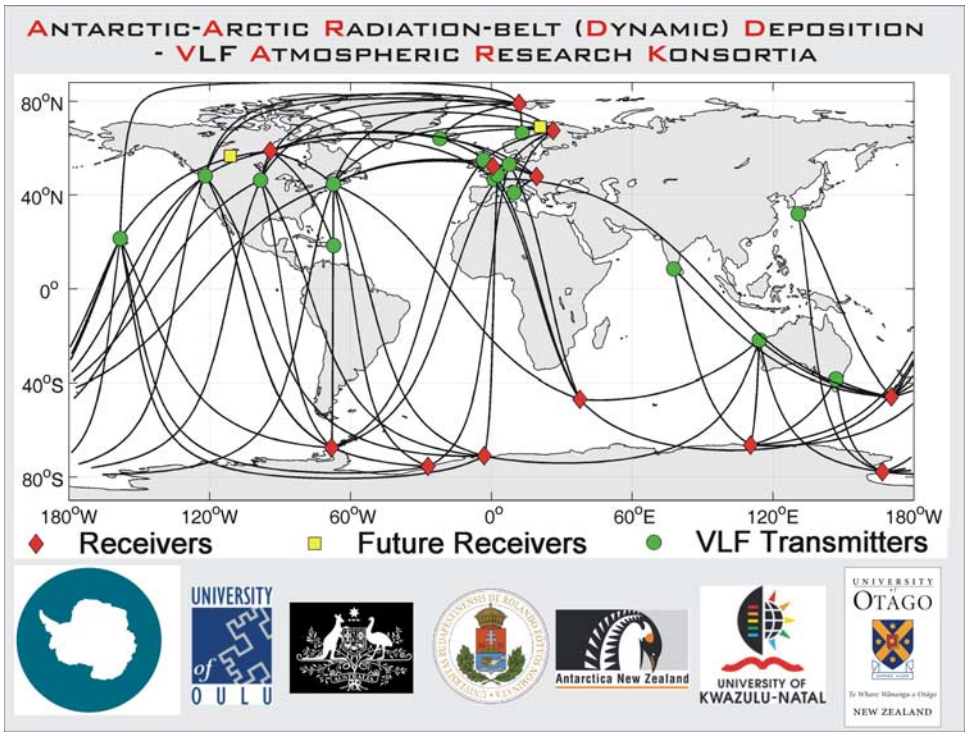

Figure 2. The great circle paths between the monitored VLF communications transmitters (T_x, green circles) and the existing AARDDVARK receiver locations (R_x, red diamonds) are shown, indicating the atmospheric areas monitored. Our planned AARDDVARK sensors for the future are shown as yellow squares.

1990]. The hardware for the receiver consists of a custom built Analog Device's ADSP-21xx Digital Signal Processor (DSP) board that resides inside a standard desktop computer. Designed in the early 1990s, DSP hardware was required for the operation of the receiver since the available desktop computers internal hardware of that time was not fast enough by itself. The DSP board has inputs for up to two broadband analog VLF signals. The input signal is immediately digitized at a 100 kHz sampling rate. The sampling rate is driven from an externally supplied precision frequency reference. From then on the rest of the receiver is implemented in software that runs on the DSP and desktop computer. The OmniPAL receiver is able to simultaneously receive up to 6 VLF transmissions. The broadband VLF signal is mixed with in-phase and quadrature phase components of a local oscillator running at the same frequency as the transmitter. The resulting in-phase and quadrature phase baseband waveforms are then low-pass filtered. Next the MSK bit clock is recovered and the signal is integrated over one bit period. The receiver incorporates a postdemodulation clipping algorithm to reduce the effect of large amplitude lightning generated impulses [*Rodger et al.*, 2007a]. The final amplitude and phase values are averaged over a specified interval of between 50 ms to 60 s and the resulting values are recorded to file on the desktop computer.

[17] The UltraMSK narrowband VLF receiver is also a software defined radio system designed to record the amplitude and phase of MSK modulated VLF radio transmissions. The receiver implements the same direct conversion radio architecture as the OmniPAL system but without the need for any custom built DSP hardware. Current desktop computing processors are now fast enough to run the UltraMSK receiver software without any additional processor support. The VLF broadband signal is sampled using readily available multichannel computer audio cards. These cards are capable of digitizing the VLF signal at sampling rates of up to 96 kHz or even 192 kHz. The receiver uses a precise 1 Pulse Per Second (PPS) signal from a GPS receiver to synthesize, in software, any required reference frequencies, removing the need for an external precision frequency reference. The number of simultaneous VLF transmissions that the receiver can record is only limited by the available computing resources. Typically, 10 or more transmitters are able to be logged with current desktop computer processors. Further information about the receiver is available on the Internet at www.ultramsk.com.

[18] The VELOX AARDVARK is a PC-based system at Casey Station, Antarctica, using LabVIEW graphical programming for data acquisition. This allows effective remote control and data visualization. The system is

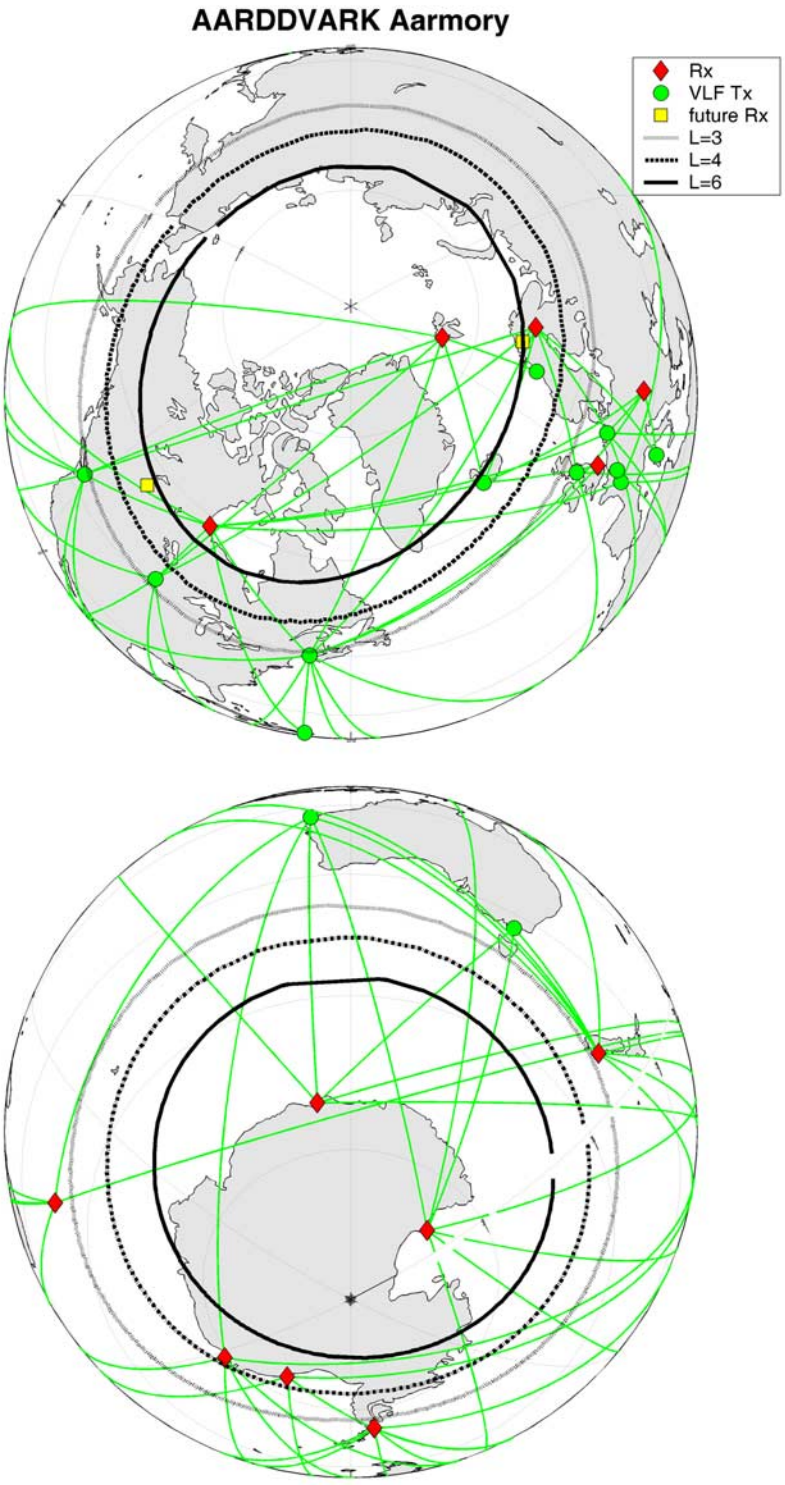

Figure 3. The AARDDVARK great circle plot maps for the northern and southern polar regions, viewed with *L* shell contours at 3, 4, and 6. Note some of the paths are quasi-constant in *L* shell.

capable of digitizing VLF signals up to 95 kHz using a DSP card. Only the amplitude of the narrowband VLF radio wave data is collected with 1-s resolution in 100 Hz bandwidth channels.

[19] Each participating institute collects and holds its own AARDDVARK data in the form of digital data sets and logs, etc. AARDDVARK members, and outside users, can request selected data periods for scientific study from one another. The exchange of AARDDVARK data from members of the Konsortia is undertaken with the goal of specific scientific projects. Data exchange is undertaken with the clear understanding that there will be coauthorship and consultation as to any publications making use of each member's data. As the AARDDVARK network is designed to monitor high-latitude events driven by processes that are often constrained by geomagnetic latitude, it is instructive to view the network in these terms. In Figure 3 we show polar projections of the great circle paths between transmitters and receivers, along with L shell contours that give some indication of the location of the auroral regions, and the footprint of the outer radiation belt.

3. Contributions to Solar Proton Event Studies

[20] The impacts of SPEs include "upsets" experienced by Earth-orbiting satellites, and increased radiation exposure levels for humans onboard spacecraft and high-altitude aircraft. AARDVVARK studies have concentrated on atmospheric ozone depletions and disruption to HF/VHF communications in mid and high-latitude regions. The most energetic SPE population deposits energy at altitudes as low as 20–30 km, producing ionization and changing the local atmospheric chemistry. SPE particles generally are at energies below which nuclear interaction losses will be significant, such that ionization-producing atmospheric interactions are the dominant energy loss. SPE-produced ionization changes tend to peak at ~73 km altitude [*Clilverd et al.*, 2005], leading to local perturbations in ozone levels [*Verronen et al.*, 2005]. Figure 4 (top) shows calculated atmospheric ionization rates at 73 km determined from the GOES-11 >10 MeV proton fluxes for the period 26 October to 7 November 2003 using output from the Sodankylä Ion and Neutral Chemistry model (SIC) [*Verronen et al.*, 2005]. Subionospheric radio wave amplitude changes received by elements of the AARDDVARK network during the October/November 2003 storms are also shown in Figure 4. These studies have shown that our understanding of VLF propagation influenced by SPEs is high, such that AARDDVARK observations might be used to predict changes in the ionospheric D region electron density profiles during other particle precipitation events [e.g., *Clilverd et al.*, 2006a]. The AARDVARK observations have been used to confirm the basic chemistry schema in the SIC model [*Clilverd et al.*, 2005; 2006b] and define more exactly the background ionization used during nondisturbed periods [*Clilverd et al.*, 2006b].

[21] Together with the SIC model, the AARDDVARK network observations have been used to investigate the destruction of odd oxygen through catalytic reactions with enhanced odd nitrogen (NO_x) and odd hydrogen (HO_x) generated by energetic particle precipitation [e.g., *Brasseur and Solomon*, 2005, pp. 291–299]. Figure 4 (bottom) shows odd oxygen changes, in particular the loss of ozone calculated by the Sodankylä Ion and Neutral Chemistry model during the October–November 2003 SPE period. While the ozone destruction at such high altitudes is generally not important to the total ozone population, under some conditions NO_x can be long lived, particularly during polar winter at high latitudes. In this situation vertical transport can drive the NO_x down toward the large ozone populations in the stratosphere, leading to large long-lived ozone depletions [e.g., *Reid et al.*, 1991]. Changes in NO_x and O_3 consistent with SPE-driven modifications have been observed [*Seppälä et al.*, 2004; *Verronen et al.*, 2005], and large depletions in ozone during the Arctic winter have been associated with a series of large SPEs over the preceding months [*Randall et al.*, 2005].

4. Contributions to Relativistic Electron Precipitation Studies

[22] Recently, subionospheric propagation probing using the AARDDVARK network observed both REP microbursts and slower REP processes, with timescales of tens of minutes, during the January 2005 "MINIS" balloon campaign [*Clilverd et al.*, 2006c]. Modeling has shown that these events are consistent with the precipitation of highly relativistic particles (>1 MeV electrons) [*Rodger et al.*, 2007a]. To the best of the authors knowledge, AARDDVARK reported the first ground based observation of microburst REP, to date unreported even by multiple balloon campaigns (e.g., MINIS) that were focused upon this goal. Estimates of flux losses due to relativistic microbursts show that they could empty the radiation belt in about a day [*Lorentzen et al.*, 2001a; *O'Brien et al.*, 2004]. Figure 5 shows an example of the AARDDVARK subionospheric VLF observations reported by *Clilverd et al.* [2006a, 2006b, 2006c]. The amplitude of multiple transmitters, received at Sodanklyä, Finland, is shown for the time period 1700–1800 UT during which the slower REP processes which occur on tens of minute scales was reported by X-ray detectors onboard the MINIS balloons. Both SLOW (timescales of tens of minutes) and FAST (short-lived spikes) are present in the subionospheric data. The FAST changes are signatures of REP microbursts. *Rodger et al.* [2007b] showed that although FAST events were observed on several paths of the Sodankylä AARDDVARK receiver very few occurred simultaneously thus indicating that the physical size of a microburst precipitation region is small and each can be thought of as a raindrop occurring as part of a larger cloud burst.

[23] REP microbursts are correlated with satellite observed VLF chorus wave activity [*Lorentzen et al.*, 2001b]. The short duration of microbursts, similar to the

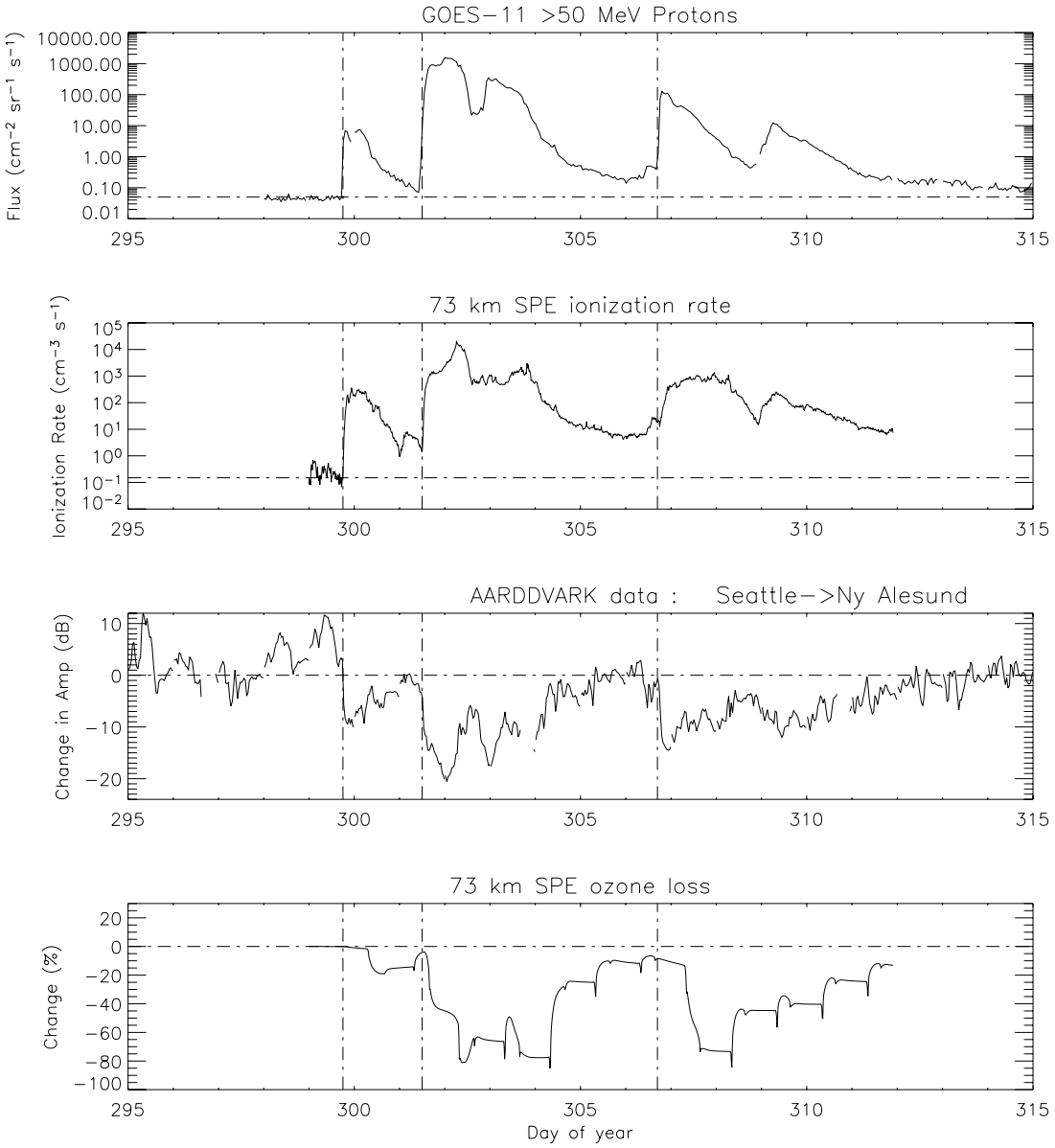

Figure 4. Showing (top) the variability of solar proton fluxes >50 MeV during the October/ November 2003 Halloween storms, the effects of the solar proton precipitation (top middle) on the ionization rate at ~73 km, and (bottom middle) on the radio wave amplitude of the VLF transmitter in Seattle (NLK) received in Ny Ålesund, Svalbard, Norway. (bottom) The percentage decreases of polar ozone at ~73 km during the same solar proton event, calculated using the Sodankylä Ion Chemistry model.

individual elements in VLF chorus, as well as the similarity in LT distributions have lead to the widely held assumption that REP microbursts are produced by wave-particle interactions with chorus waves. However, this has yet to be confirmed, and a one-to-one correlation of REP microbursts and chorus elements has yet to be demonstrated. Because of the integral flux detectors present onboard SAMPEX, limited information on the energy spectra of REP microbursts has been available to date. Ground based AARDDVARK observations of REP microbursts confirm the highly energetic spectra, where the peak electron precipitation fluxes are ~2 MeV, but this is not particularly consistent with the calculated energy spectra expected for precipitation from resonance with chorus waves [*Rodger et al.*, 2006]. However, this may indicate the very difficult task of adequately modeling the interaction of VLF chorus

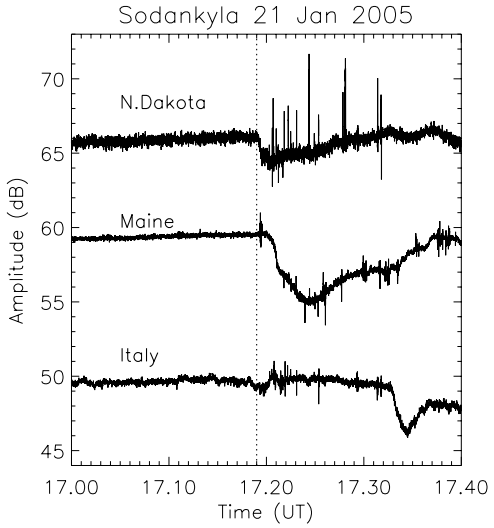

Figure 5. Showing the effects of energetic electron precipitation, during a magnetospheric shock event driven by a coronal mass ejection, on radio wave amplitudes received at Sodankylä, Finland ($L = 5$). Both short and long timescale amplitude perturbations (i.e., particle precipitation) signatures are observed.

waves with energetic radiation belt particles during geomagnetic storms. Nonetheless, the satellite and VLF subionospheric measurements confirm the extremely high-energy nature of relativistic microbursts.

[24] In addition to REP microbursts there is also another REP phenomena (termed SLOW events), in which REP occurs in long-lived bursts. Precipitation events lasting minutes to hours have been observed from the MAXIS balloon, where they typically occur at about $L = 4-7$, are observed in the late afternoon/dusk sector, and may be produced by electromagnetic ion cyclotron waves [*Millan et al.*, 2002]. Loss rates suggest that these minute-hour events may be the primary loss mechanism for outer zone relativistic electrons. *Clilverd et al.* [2006a, 2006b, 2006c] recently examined these SLOW REP using AARDDVARK data, focusing on the total trapped flux lost into the atmosphere. Their study focused on the sudden electron flux decrease of 1700 UT on 21 January 2005. The event shows similar local time dependence and flux level changes as those reported by *Onsager et al.* [2002] and *Green et al.* [2004]. The AARDDVARK-based study concluded that $\sim$1/2 of the sudden electron flux decrease precipitates into the atmosphere over 2.7 h, between $L = 4$ and 6 [*Clilverd et al.*, 2006a, 2006b, 2006c]. Both FAST and SLOW processes result in loss of outer radiation belt particles, often during the same geomagnetic storm.

5. Contributions to the Studies of Descending NO_x

[25] Subionospheric VLF radio wave propagation is sensitive to ionization located below about 90 km, including that produced by the ionization of NO_X by Lyman-α [*Solomon et al.*, 1982b]. The effect of increased ionization on the propagating signals can be seen as either an increase or decrease in signal amplitude or phase depending on the modal mixture of each signal observed. From the changes in ionospheric propagation conditions during the winter period we can determine the levels of mesospheric NO_X either through in situ production or descent from the thermosphere. The descent of NO_X into the altitude region in which AARDDVARK measurements are sensitive is controlled by vertical transport within the high-latitude polar vortex. Descending NO_X causes destruction of mesospheric and stratospheric ozone, and therefore influences the radiation budget of the atmosphere, driving changes in stratospheric circulation and temperature.

[26] In several recent studies we have analyzed AARDDVARK data from midhigh latitudes during the northern polar winters of 2003–2004, 2004–2005, and 2005–2006 [*Clilverd et al.*, 2005, 2006a, 2007]. Significant variability is observed in the overall levels of either the daytime or nighttime propagation conditions, particularly resulting in changes in received amplitude. The 3 years studied showed significant differences in solar activity, and stratospheric vortex strength, allowing us to study the interplay between these two parameters. The AARDDVARK data sets are available to the researchers involved in real time, are easy to analyze for this effect, thus making them an important tool in the investigation of solar activity influences on the middle atmosphere. Figure 6 includes the latest data from Ny Ålesund (i.e., up to the date of 20 April 2008), showing the changing winter time day-night propagation conditions caused by direct particle precipitation below the ionosphere (shown by solid vertical lines), or by enhanced NO_X (dotted vertical lines). Note the lack of recent events due to the proximity of 11-year solar cycle minimum.

[27] Over recent years there has been significant discussion about the altitude at which descending NO_X is generated, as this could identify the source mechanism. Many papers have discussed the events of the northern hemisphere winter 2003–2004. Although several powerful solar storms occurred at the beginning of the 2003–2004 winter period (October and November) the main cause of the descending NO_X observed at the end of the winter period was uncertain because of the breakup of the stratospheric vortex in late December 2003. *Renard et al.* [2006] suggested that the source of descending NO_X was in situ production at around 60 km caused by electrons of a few hundred keV, due to a geomagnetic storm that occurred on 22–25 January 2004. However, *Clilverd et al.* [2006a] used AARDDVARK data to show that the primary source altitude for the NO_X in this time period was the auroral zones in the thermosphere, and not a result of in situ production in the mesosphere. The descent of the NO_X began a few days after the end of the stratospheric warming event at the end of December 2003. In that study

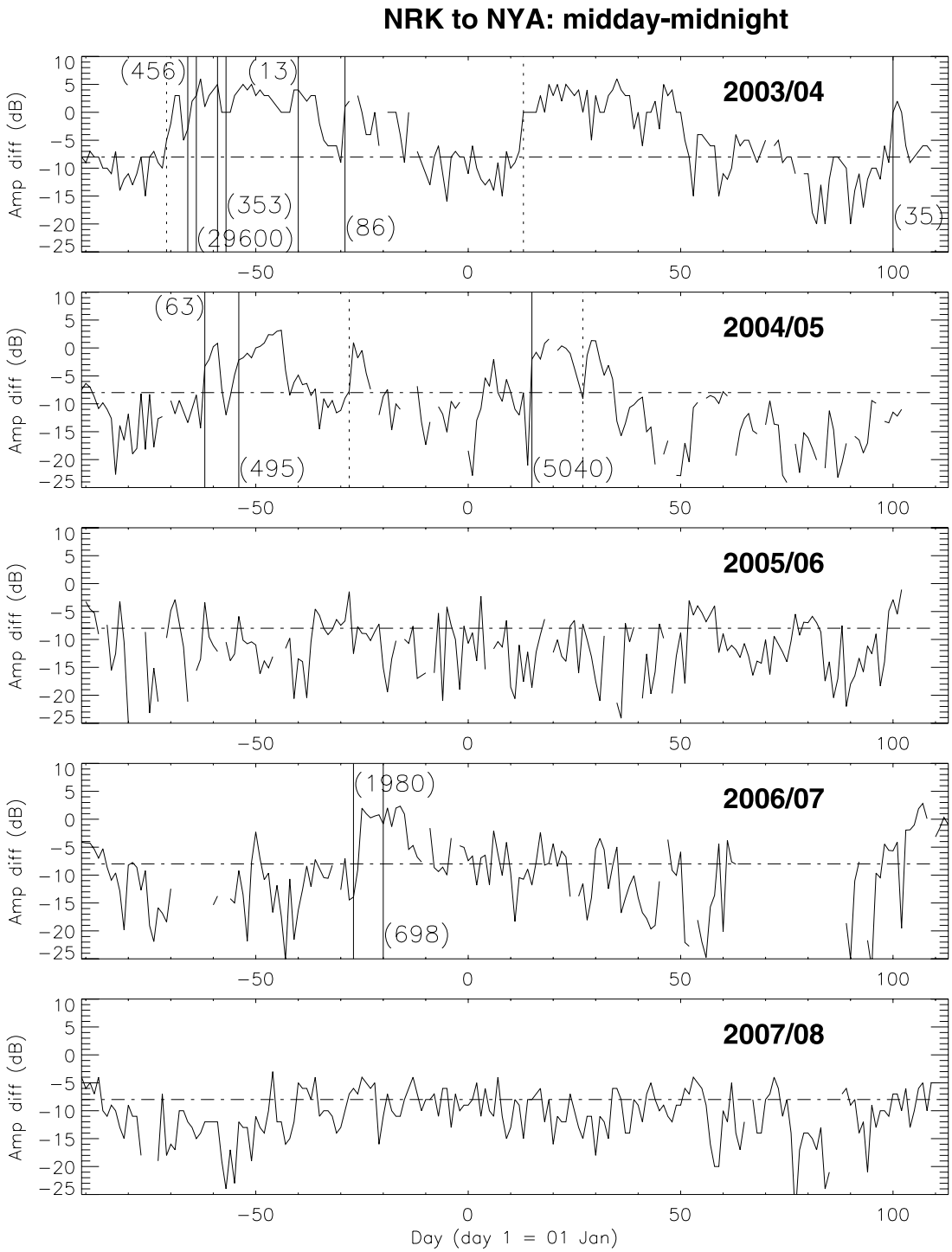

Figure 6. Winter time AARDDVARK data from Ny Ålesund, Svalbard, using the Iceland transmitter (NRK, 37.5 kHz) taken over 5 years. The radio wave index is shown, representing the amplitude difference between average midday and midnight propagation conditions, with solid vertical lines representing times of changed ionization conditions due to solar proton events (with the peak >10 MeV fluxes in brackets), and the dashed vertical lines representing ionization changes caused by the descent of odd nitrogen (NO_X) from the thermosphere.

it was unclear whether the thermospheric reservoir of high-altitude NO_X was generated by the large solar storms several months earlier, or by an accumulation of the effects of smaller storms as suggested by *Siskind* [2000].

[28] Using a combination of AARDDVARK data and GOMOS satellite observations of NO_2 *Seppälä et al.* [2007] showed that there were several contributions to the NO_X/ozone variations during the winter 2003–2004. One significant source of NO_X was the thermosphere, generated by nonrelativistic electron precipitation, while solar proton precipitation from solar storms, and relativistic electron precipitation driven by geomagnetic storms were also significant at various times across this period. These mechanisms produce NO_X at different altitudes, and over different timescales so the combined effect on the ozone population is incomplete and still needs clarification. All of these mechanisms produce well defined effects in AARDDVARK data, and those observations can be used to determine the precipitation energy spectra and describe the underlying physical processes that cause the precipitation [*Turunen et al.*, 2009].

6. Contributions to Solar Flare Studies

[29] For daytime solar flares, both the D region height lowering and the subsequent phase advance of VLF signals (at least for path lengths greater than a few Mm) have been found to be nearly proportional to the logarithm of the X-ray flux [*McRae and Thomson*, 2004]. Many of the propagation paths monitored by the AARDDVARK network are sensitive to solar flare effects because they often monitor long transequatorial paths. An extensive data set of flare events has already been recorded. In addition, the network paths are sensitive to the massive effects of magnetars [*Inan et al.*, 1999], with several already captured in archive data.

[30] Unlike GOES X-ray flux measurements made from geosynchronous orbit, D region flare-induced ionospheric changes show no saturation effects, even for very large flares [*Thomson et al.*, 2004], and therefore allow the study of extreme solar events. The received VLF phase changes can be used to measure the X-ray fluxes, even though GOES X-ray fluxes have may have reached saturation, and determine the peak levels. *Thomson et al.* [2004, 2005] used this technique on the 4 November 2003 flare event, combining GOES fluxes in the band 0.1–0.8 nm together with the AARDDVARK data from daytime VLF paths across the Pacific to Dunedin, New Zealand, including the transmitters NLK (Seattle, 24.8 kHz), NPM (Hawaii, 21.4 kHz), and NDK (North Dakota, 25.2 kHz). They found that the technique gave a magnitude of X45 ± 5 (4.5 ± 0.5 mW/m^2 in the 0.1–0.8 nm band) for the great flare as compared with the value of X28 (2.8 mW/m^2 in the 0.1–0.8 nm band) estimated by NOAA's Space Environment Center (SEC) (http://sec.noaa.gov/weekly/pdf2003/prf1471.pdf) derived from GOES measurements which saturated at ~X20. The great X45 flare is the largest yet measured. This work showed that solar flares can be more extreme than previously thought. Figure 7 shows an example of a comparison between a series of both strong and weak solar flares seen in GOES X-ray flux data and the VLF subionospheric measurements from the transmitters NWC (North West Cape, Australia), NTS (Sale, Australia) and JAP (Japan) observed at Casey, Antarctica. The AARDDVARK network is able to monitor solar flare activity because of its comprehensive longitude coverage, always ensuring that some paths are on the day side of the Earth.

7. Future Expansion Plans

[31] As indicated in Figure 2 the AARDDVARK network is likely to expand in the near future to include several more receiving stations, and thus increase the local time coverage of subionospheric propagation conditions in both the northern and southern hemispheres. With the potential for upcoming satellite missions to investigate acceleration and loss processes in the Van Allen belts (RBSP, ORBITALS, ERG) the AARDDVARK network is perfectly positioned to provide high time resolution, continuous particle precipitation data that will enhance the understanding of the physical loss processes taking place.

[32] AARDDVARK data will also support the NASA funded BARREL (Balloon Array for Radiation-belt Relativistic Electron Losses) experiment that will be undertaken in 2012 with a view to investigate relativistic electron precipitation processes. The combination of AARDDVARK data and the MINIS balloon X-ray flux data, during an intense geomagnetic storm associated with a coronal mass ejection from the Sun has already shown the value of the network [*Clilverd et al.*, 2007]. The AARDDVARK network also overlaps regions where there are substantial arrays of riometers well positioned to provide point measurements of overhead ionization conditions, e.g., GLORIA and NORSTAR [*Spanswick et al.*, 2005]. The combination of these two experimental techniques allows improved resolution of the energy spectra of precipitating fluxes.

[33] Future expansions of the AARDDVARK network will highlight quasi-constant L shell propagation paths to provide clearer description of the precipitation processes occurring within well-defined regions of the magnetosphere. The strength of the quasi-constant L shell propagation path analysis was shown by the observations of long-term precipitation caused by plasmaspheric hiss after an outer radiation belt injection into $L = 3$ [*Rodger et al.*, 2007b]. Future expansion will also allow global coverage of space weather events, rather than the limited coverage currently available. Expanding into the southern hemisphere is a particular problem for the experimental observations, but combined solar- and wind-powered systems are being considered for the near future.

8. Summary

[34] The Antarctic-Arctic Radiation-belt (Dynamic) Deposition-VLF Atmospheric Research Konsortium is a global network of radio receivers designed to make

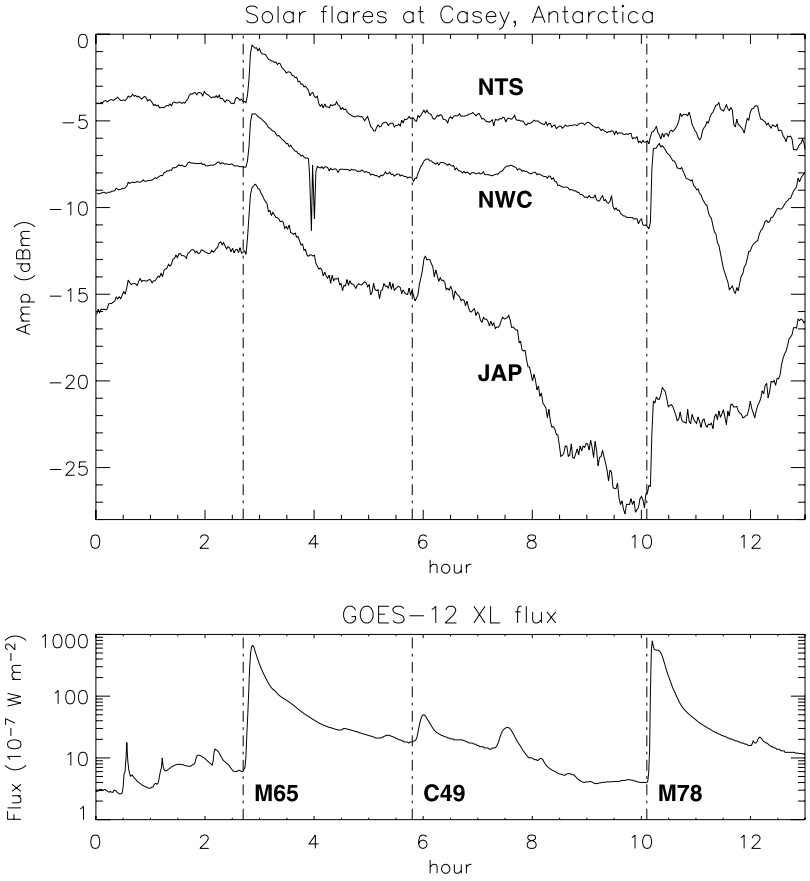

Figure 7. Example of a sequence of solar flares on 2 December 2005 observed at Casey, Antarctica, on three separate paths from Australia and Japan, shown in amplitude along with the coincident GOES 0.1−0.8 nm X-ray fluxes and flare classifications.

continuous long-range observations of the lower ionosphere at mid to high-latitude regions. The network of cheap, easy to install, easy to maintain sensors are used to detect changes in ionization levels from ~30−90 km altitude, ultimately sensing pace weather events globally, continuously, and with high time resolution. All with the goal of increasing the understanding of energy coupling between the Earth's atmosphere, the Sun, and space.

[35] The AARDDVARK network has contributed to the scientific understanding of an increasing list of space weather science topics, including the chemical modification of the middle atmosphere during solar proton events, the precipitation mechanisms of relativistic electrons, the descent of NO_x into the middle atmosphere, and the effects of large solar flares. These science areas impact our knowledge of space weather processes, global atmospheric change, communications, and navigation. Future expansions of the network will increase the science potential and provide global coverage of space weather event signatures.

[36] **Acknowledgments.** The authors would like to thank the staff at Churchill (Churchill Northern Studies Center), Casey (Australian Antarctic Division project ASAC 1324), and Ny Ålesund (Natural Environment Research Council) for their assistance in operating the AARDDVARK receivers at those sites. We would also like to acknowledge the efforts of the BAS winterers at Halley and Rothera bases (Antarctica) in operating the AARDDVARK systems there. The analysis and interpretation of AARDDVARK data has been supported by funding from the Finnish Academy.

References

Adams, C. D. D., and R. L. Dowden (1990), VLF group delay of lightning-induced electron-precipitation echoes from measurement of phase and amplitude perturbations at 2 frequencies, *J. Geophys. Res.*, *95*, 2457−2462, doi:10.1029/JA095iA03p02457.

Bainbridge, G., and U. S. Inan (2003), Ionospheric D region electron density profiles derived from the measured interference pattern of VLF waveguide modes, *Radio Sci.*, *38*(4), 1077, doi:10.1029/2002RS002686.

Barr, R., D. L. Jones, and C. J. Rodger (2000), ELF and VLF radio waves, *J. Atmos. Sol. Terr. Phys.*, *62*, 1689−1718, doi:10.1016/S1364-6826(00)00121-8.

Bichel, J. E., J. L. Heritage, and S. Weisbrod (1957), An experimental measurement of VLF field strength as a function of distance using an aircraft, *Rep. 767*, Navy Electron. Lab., San Diego, Calif.

Blake, J. B., M. D. Looper, D. N. Baker, R. Nakamura, B. Klecker, and D. Hovestadt (1996), New high temporal and spatial resolution measurements by SAMPEX of the precipitation of relativistic electrons, *Adv. Space Res.*, *18*(8), 171–186, doi:10.1016/0273-1177(95)00969-8.

Bracewell, R. N., K. G. Budden, J. A. Ratcliffe, T. W. Straker, and K. Weeks (1951), The ionospheric propagation of low and very-low frequency radio waves over distances less than 1000 km, *Proc. IEEE*, *98*, 221–236.

Brasseur, G., and S. Solomon (2005), *Aeronomy of the Middle Atmosphere*, 3rd ed., D. Reidel, Dordrecht, Netherlands.

Budden, K. G. (1955), The numerical solution of differential equations governing reflection of long radio waves from the ionosphere, *Proc. R. Soc. London Ser. A*, *227*, 516–537, doi:10.1098/rspa.1955.0027.

Cane, H. V., T. T. von Rosenvinge, C. M. S. Cohen, and R. A. Mewaldt (2003), Two components in major solar particle events, *Geophys. Res. Lett.*, *30*(12), 8017, doi:10.1029/2002GL016580.

Clilverd, M. A., C. J. Rodger, T. Ulich, A. Seppälä, E. Turunen, A. Botman, and N. R. Thomson (2005), Modeling a large solar proton event in the southern polar atmosphere, *J. Geophys. Res.*, *110*, A09307, doi:10.1029/2004JA010922.

Clilverd, M. A., A. Seppälä, C. J. Rodger, P. T. Verronen, and N. R. Thomson (2006a), Ionospheric evidence of thermosphere-to-stratosphere descent of polar NO_X, *Geophys. Res. Lett.*, *33*, L19811, doi:10.1029/2006GL026727.

Clilverd, M. A., A. Seppälä, C. J. Rodger, N. R. Thomson, P. T. Verronen, E. Turunen, T. Ulich, J. Lichtenberger, and P. Steinbach (2006b), Modeling polar ionospheric effects during the October–November 2003 solar proton events, *Radio Sci.*, *41*, RS2001, doi:10.1029/2005RS003290.

Clilverd, M. A., C. J. Rodger, and T. Ulich (2006c), The importance of atmospheric precipitation in storm-time relativistic electron flux drop outs, *Geophys. Res. Lett.*, *33*, L01102, doi:10.1029/2005GL024661.

Clilverd, M. A., A. Seppälä, C. J. Rodger, N. R. Thomson, J. Lichtenberger, and P. Steinbach (2007), Temporal variability of the descent of high-altitude NO_X inferred from ionospheric data, *J. Geophys. Res.*, *112*, A09307, doi:10.1029/2006JA012085.

Crombie, D. D. (1964), Periodic fading of VLF signals received over long paths during sunrise + sunset, *J. Res. Natl. Bur. Stand.*, *68D*, 27–37.

Cummer, S. A. (2000), Modeling electromagnetic propagation in the earth-ionosphere waveguide, *IEEE Trans. Antennas Propag.*, *48*(9), 1420–1429, doi:10.1109/8.898776.

Deeks, D. G. (1966a), D-region electron distributions in middle latitudes deduced from the reflection of long radio waves, *Proc. R. Soc. London Ser. A*, *291*, 413–437, doi:10.1098/rspa.1966.0103.

Deeks, D. G. (1966b), Generalised full wave theory for energy dependent collision frequencies, *J. Atmos. Terr. Phys.*, *28*, 839–846.

Dowden, R. L., S. F. Hardman, C. J. Rodger, and J. B. Brundell (1998), Logarithmic decay and Doppler shift of plasma associated with sprites, *J. Atmos. Sol. Terr. Phys.*, *60*, 741–753, doi:10.1016/S1364-6826(98)00019-4.

Ferguson, J. A., and F. P. Snyder (1990), Computer programs for assessment of long wavelength radio communications, *Tech. Doc. 1773*, Natl. Ocean Syst. Cent., San Diego, Calif.

Green, J. C., T. G. Onsager, T. P. O'Brien, and D. N. Baker (2004), Testing loss mechanisms capable of rapidly depleting relativistic electron flux in the Earth's outer radiation belt, *J. Geophys. Res.*, *109*, A12211, doi:10.1029/2004JA010579.

Hollingworth, J. (1926), The propagation of radio waves, *IEEE*, *46*, 579–595.

Imhof, W. L., H. D. Voss, J. Mobilia, M. Walt, U. S. Inan, and D. L. Carpenter (1989), Characteristics of short-duration electron precipitation bursts and their relationship with VLF wave activity, *J. Geophys. Res.*, *94*, 10,079–10,093, doi:10.1029/JA094iA08p10079.

Inan, U., N. Lehtinen, S. Lev-Tov, M. Johnson, T. Bell, and K. Hurley (1999), Ionization of the lower ionosphere by γ-rays from a magnetar: Detection of a low energy (3–10 keV) component, *Geophys. Res. Lett.*, *26*(22), 3357–3360, doi:10.1029/1999GL010690.

Kennelly, A. E. (1902), On the elevation of the electrically conducting strata of the earth's atmosphere, *Electr. World Eng.*, *39*, 8–12.

Krucker, S., and R. P. Lin (2000), On the solar release of energetic particles detected at 1 AU: Acceleration and transport of energetic particles observed in the heliosphere, *AIP Conf. Proc.*, *528*, 87–90.

Lorentzen, K. R., J. B. Blake, U. S. Inan, and J. Bortnik (2001a), Observations of relativistic electron microbursts in association with VLF chorus, *J. Geophys. Res.*, *106*(A4), 6017–6027, doi:10.1029/2000JA003018.

Lorentzen, K. R., M. D. Looper, and J. B. Blake (2001b), Relativistic electron microbursts during the GEM storms, *Geophys. Res. Lett.*, *28*(13), 2573–2576, doi:10.1029/2001GL012926.

Magono, C. (1980), *Thunderstorms*, Elsevier, Amsterdam.

McRae, W. M., and N. R. Thomson (2000), VLF phase and amplitude: Daytime ionospheric parameters, *J. Atmos. Sol. Terr. Phys.*, *62*(7), 609–618, doi:10.1016/S1364-6826(00)00027-4.

McRae, W. M., and N. R. Thomson (2004), Solar flare induced ionospheric D-region enhancements from VLF phase and amplitude observations, *J. Atmos. Sol. Terr. Phys.*, *66*(1), 77–87, doi:10.1016/j.jastp.2003.09.009.

Millan, R. M., R. P. Lin, D. M. Smith, K. R. Lorentzen, and M. P. McCarthy (2002), X-ray observations of MeV electron precipitation with a balloon-borne germanium spectrometer, *Geophys. Res. Lett.*, *29*(24), 2194, doi:10.1029/2002GL015922.

O'Brien, T. P., M. D. Looper, and J. B. Blake (2004), Quantification of relativistic electron microburst losses during the GEM storms, *Geophys. Res. Lett.*, *31*, L04802, doi:10.1029/2003GL018621.

Onsager, T. G., G. Rostoker, H.-J. Kim, G. D. Reeves, T. Obara, H. J. Singer, and C. Smithtro (2002), Radiation belt electron flux dropouts: Local time, radial, and particle-energy dependence, *J. Geophys. Res.*, *107*(A11), 1382, doi:10.1029/2001JA000187.

Piggott, W. R., M. L. V. Pitteway, and E. V. Thrane (1965), The numerical calculation of wave-fields, reflection coefficients, and polarizations for long radio waves in the lower ionosphere II, *Philos. Trans. R. Soc. London Ser. A*, *257*, 243–271, doi:10.1098/rsta.1965.0005.

Pitteway, M. L. V. (1965), The numerical calculation of wave-fields, reflection coefficients, and polarizations for long radio waves in the lower ionosphere I, *Philos. Trans. R. Soc. London Ser. A*, *257*, 219–241, doi:10.1098/rsta.1965.0004.

Popov, A. S. (1896), Instrument for detection and registration of electrical fluctuations, *J. Russ. Phys. Chem. Soc.*, *1*, 1–14.

Randall, C. E., et al. (2005), Stratospheric effects of energetic particle precipitation in 2003–2004, *Geophys. Res. Lett.*, *32*, L05802, doi:10.1029/2004GL022003.

Reeves, G. D. (1998), Relativistic electrons and magnetic storms: 1992–1995, *Geophys. Res. Lett.*, *25*(11), 1817–1820, doi:10.1029/98GL01398.

Reeves, G. D., T. E. Cayton, S. P. Gary, and R. D. Belan (1992), The great solar energetic particle events of 1989 observed from geosynchronous orbit, *J. Geophys. Res.*, *97*, 6219–6226, doi:10.1029/91JA03102.

Reid, G. C., S. Solomon, and R. R. Garcia (1991), Response of the middle atmosphere to solar proton events of August–December, 1989, *Geophys. Res. Lett.*, *18*, 1019–1022, doi:10.1029/91GL01049.

Renard, J.-B., P.-L. Blelly, Q. Bourgeois, M. Chartier, F. Goutail, and Y. J. Orsolini (2006), Origin of the January–April 2004 increase in stratospheric NO_2 observed in the northern polar latitudes, *Geophys. Res. Lett.*, *33*, L11801, doi:10.1029/2005GL025450.

Rodger, C. J., M. A. Clilverd, P. T. Verronen, T. Ulich, M. J. Jarvis, and E. Turunen (2006), Dynamic geomagnetic rigidity cutoff variations during a solar proton event, *J. Geophys. Res.*, *111*, A04222, doi:10.1029/2005JA011395.

Rodger, C. J., M. A. Clilverd, D. Nunn, P. T. Verronen, J. Bortnik, and E. Turunen (2007a), Storm time, short-lived bursts of relativistic electron precipitation detected by subionospheric radio wave propagation, *J. Geophys. Res.*, *112*, A07301, doi:10.1029/2007JA012347.

Rodger, C. J., M. A. Clilverd, N. R. Thomson, R. J. Gamble, A. Seppälä, E. Turunen, N. P. Meredith, M. Parrot, J. A. Sauvaud, and J.-J. Berthelier (2007b), Radiation belt electron precipitation into the atmosphere: Recovery from a geomagnetic storm, *J. Geophys. Res.*, *112*, A11307, doi:10.1029/2007JA012383.

Round, H. J., T. L. Eckersley, K. Tremellen, and F. C. Lunnon (1925), Report on measurements made on signal strength at great distances during 1922 and 1923 by an expedition sent to Australia, *J. IEE*, *63*(346), 62.

Seppälä, A., P. T. Verronen, E. Kyrölä, S. Hassinen, L. Backman, A. Hauchecorne, J. L. Bertaux, and D. Fussen (2004), Solar proton events of October–November 2003: Ozone depletion in the Northern hemisphere polar winter as seen by GOMOS/Envisat, *Geophys. Res. Lett.*, *31*, L19107, doi:10.1029/2004GL021042.

Seppälä, A., M. A. Clilverd, and C. J. Rodger (2007), NO_X enhancements in the middle atmosphere during 2003–2004 polar winter: Relative significance of solar proton events and the aurora as a source, *J. Geophys. Res.*, *112*, D23303, doi:10.1029/2006JD008326.

Shea, M. A., and D. F. Smart (1990), A summary of major solar proton events, *Sol. Phys.*, *127*(2), 297–320, doi:10.1007/BF00152170.

Siskind, D. E. (2000), On the coupling between the middle and upper atmospheric odd nitrogen, in *Atmospheric Science Across the Stratopause, Geophys. Monogr. Ser.*, vol. *123*, edited by D. E. Siskind, S. D. Eckermann, and M. E. Summers, pp. 101–116, AGU, Washington, D. C.

Solomon, S., P. J. Crutzen, and R. G. Roble (1982a), Photochemical coupling between the thermosphere and the lower atmosphere: 1. Odd nitrogen from 50 to 120 km, *J. Geophys. Res.*, *87*, 7206–7220, doi:10.1029/JC087iC09p07206.

Solomon, S., G. C. Reid, R. G. Roble, and P. J. Crutzen (1982b), Photochemical coupling between the thermosphere and the lower atmosphere: 2. D-region ion chemistry and the winter anomaly, *J. Geophys. Res.*, *87*, 7221–7227, doi:10.1029/JC087iC09p07221.

Sommerfeld, A. (1909), Über die ausbreitung der wellen in der drahtlosen telegraphie, *Ann. Phys.*, *28*, 665–736, doi:10.1002/andp.19093330402.

Spanswick, E., E. Donovan, and G. Baker (2005), Pc5 modulation of high energy electron precipitation: Particle interaction regions and scattering efficiency, *Ann. Geophys.*, *23*, 1533–1542.

Straker, T. W. (1955), The ionospheric reflection of radio waves of frequency 16 kc/s over short distances, *Proc. IEEE*, *102C*, 396.

Thomson, N. R., C. J. Rodger, and R. L. Dowden (2004), Ionosphere gives size of greatest solar flare, *Geophys. Res. Lett.*, *31*, L06803, doi:10.1029/2003GL019345.

Thomson, N. R., C. J. Rodger, and M. A. Clilverd (2005), Large solar flares and their ionospheric D region enhancements, *J. Geophys. Res.*, *110*, A06306, doi:10.1029/2005JA011008.

Thomson, N. R., M. A. Clilverd, and W. M. McRae (2007), Nighttime ionospheric D region parameters from VLF phase and amplitude, *J. Geophys. Res.*, *112*, A07304, doi:10.1029/2007JA012271.

Turunen, E., H. Matveinen, J. Tolvanen, and H. Ranta (1996), D-region ion chemistry model, in *STEP Handbook of Ionospheric Models*, edited by R. W. Schunk, pp. 1–25, SCOSTEP Secr., Boulder, Colo.

Turunen, E., P. T. Verronen, A. Seppälä, C. J. Rodger, M. A. Clilverd, J. Tamminen, C.-F. Enell, and T. Ulich (2009), Impact of different precipitation energies on NOx generation during geomagnetic storms, *J. Atmos. Sol. Terr. Phys.*, in press.

Verronen, P. T., A. Seppälä, M. A. Clilverd, C. J. Rodger, E. Kyrölä, C. Enell, T. Ulich, and E. Turunen (2005), Diurnal variation of ozone depletion during the October–November 2003 solar proton events, *J. Geophys. Res.*, *110*, A09S32, doi:10.1029/2004JA010932.

Wait, J. R. (1963), Concerning solutions of the V. L. F. mode problem for an anisotropic curved ionosphere, *J. Res. Natl. Bur. Stand.*, *67D*, 297–302.

Watt, A. D. (1967), VLF radio engineering, in *Electromagnetic Waves*, vol. *14*, edited by A. L. Cullen, V. A. Fock, and J. R. Wait, chapter 3, pp. 171–394, Pergamon Press, New York.

Weeks, K. (1950), The ground interference pattern of very-low-frequency radio waves, *Proc. IEE*, *97*(III), 100–107.

J. B. Brundell, UltraMSK.com, Dunedin, New Zealand. (james@brundell.co.nz)

M. A. Clilverd and N. Cobbett, Physical Sciences Division, British Antarctic Survey, High Cross, Madingley Road, Cambridge CB3 0ET, UK. (macl@bas.ac.uk; nco@bas.ac.uk)

A. B. Collier, Hermanus Magnetic Obsevatory, P.O. Box 32, Hermanus 7200, South Africa. (abcollier@hmo.ac.za)

J. Lichtenberger, Space Research Group, Eötvös University, Budapest H 1518, Hungary. (spacerg@sas.elte.hu)

F. W. Menk, School of Mathematical and Physical Sciences and Cooperative Research Centre for Satellite Systems, University of Newcastle, Callaghan, NSW 2308, Australia. (fred.menk@newcastle.edu.au)

C. J. Rodger and N. R. Thomson, Department of Physics, University of Otago, P.O. Box 56, Dunedin 9016, New Zealand. (crodger@physics.otago.ac.nz; n_thomson@physics.otago.ac.nz)

A. Seppälä and P. T. Verronen, Earth Observation, Finnish Meteorological Institute, P.O. Box 503, FIN-00101 Helsinki, Finland. (annika.seppala@fmi.fi; pekka.verronen@fmi.fi)

E. Turunen and T. Ulich, Sodankylä Geophysical Observatory, University of Oulu, Tähteläntie 62, FIN-99600 Sodankylä, Finland. (esa@sgo.fi; thu@sgo.fi)